

COOLING CHARACTERISTICS OF PWR-TYPE FUEL ELEMENT SIMULATORS TESTED IN THE QUENCH EXPERIMENTS

L. Sepold, A. Miassoedov, M. Steinbrück, J. Stuckert
Forschungszentrum Karlsruhe (Karlsruhe Research Center)
Institut für Materialforschung
P.O. Box 3640, 76021 Karlsruhe, Federal Republic of Germany
Email leo.sepold@imf.fzk.de

KEY WORDS

Cooling by water and steam injection, core reflooding behavior, out-of-pile bundle experiments, LWR severe accident research.

ABSTRACT

The QUENCH out-of-pile experiments at the Karlsruhe Research Center are carried out to investigate the hydrogen source term resulting from reflooding an uncovered core of a light-water reactor for cooling. They also are to improve understanding of the effects of water injection at different stages of a degraded core, and to create a data base for model development and code improvement. Under certain circumstances, water injection can cause renewed, enhanced oxidation of the zircaloy cladding, at the same time rapidly raising both the temperature and hydrogen generation as a consequence of the extensive exothermal zirconium-steam reaction. This phenomenon was demonstrated before in analyses of the TMI-2 accident and in results of the CORA out-of-pile and LOFT LP-FP-2 in-pile experiments.

One of the main parameters of the test program is the quenching medium, i.e. water or steam, both injected from the bottom. Injection from the top is planned for future experiments. Up to now, eight QUENCH experiments have been performed with and without a B₄C absorber.

The test bundle consists of 21 fuel rod simulators, 20 of which are electrically heated over a length of 1024 mm. The central rod is unheated, i.e. it is either a fuel rod simulator or a control rod simulator with a B₄C absorber rod. The Zircaloy-4 rod claddings and the grid spacers are identical to those used in pressurized water reactors, whereas the fuel is represented by ZrO₂ pellets. The test section is instrumented with thermocouples attached to the cladding, the shroud, and the double-walled cooling jacket at levels between -50 mm and 1350 mm. Three out of four corner rods each are equipped with a centerline thermocouple.

After an optional pre-oxidation phase in an argon/steam flow the test bundle is heated in the transient phase at an initial heating rate of ~0.1 K/s. A consequence of the temperature rise, the test bundle normally experiences a temperature excursion due to the exothermal zirconium-steam reaction. This temperature excursion usually begins at the 850-950 mm level at around 1773 K, leading to the maximum bundle temperature and increased hydrogen generation. The flooding phase is initiated when the test bundle temperature is well above 2000 K. The quenching water is injected at a rate of 1.3-1.7 cm/s, corresponding to approx.

50 g/s. The steam injection rate is 50 or 15 g/s. With progressive cooling, hydrogen generation either stops almost immediately, or continues, or even increases, as was the case in four out of eight QUENCH experiments.

From the very beginning of the cooling phase, quenching the bundle with water leads to cooling under two-phase flow conditions because the injected water turns into steam already at lower levels. Cooling occurs in two stages, first, a moderate cooling stage where heat is transferred from the bundle to the coolant under film boiling conditions, followed by a very pronounced cooling stage due to heat transfer by transition and nucleate boiling. In the upper half of the bundle pronounced cooling is delayed so much that a steam flow with water droplets fills the coolant channels longer than it does at lower levels. Under film boiling conditions at the upper levels, the test bundle cools in a similar way as the entire bundle length does when steam is injected instead of water. Cooling rates differ not only for water and steam injection, but also for lower and upper bundle levels in case of water quenching. They are at a maximum for water quenching, particularly during the period of pronounced cooling in the lower half of the test bundle, i.e. when the rod surfaces there begin to be wetted.

Evaluation of the progression of the wetting front was based on the evolution of complete wetting in the axial direction, i.e. on the first indication of thermocouples reaching saturation temperature. In the QUENCH-01, -03, and -06 experiments, the wetting front progresses at a rate of approx. 0.5-0.6 cm/s from 50 to 500 mm.

Three independent methods, i.e. (a) steam measurements by mass spectrometer, (b) differential pressure data of the orifice located in the offgas pipe, and (c) condensate collector data, were used to evaluate the evaporation resulting from injection of quenching water into the hot test bundle. An evaporation ratio, i.e. the mass flow of steam produced relative to that of water injected, was evaluated on the basis of QUENCH-06 data. This ratio seems to change mainly during the first 70-80 s of the quenching phase and then stay constant for the rest of the flooding phase at roughly 35 %.

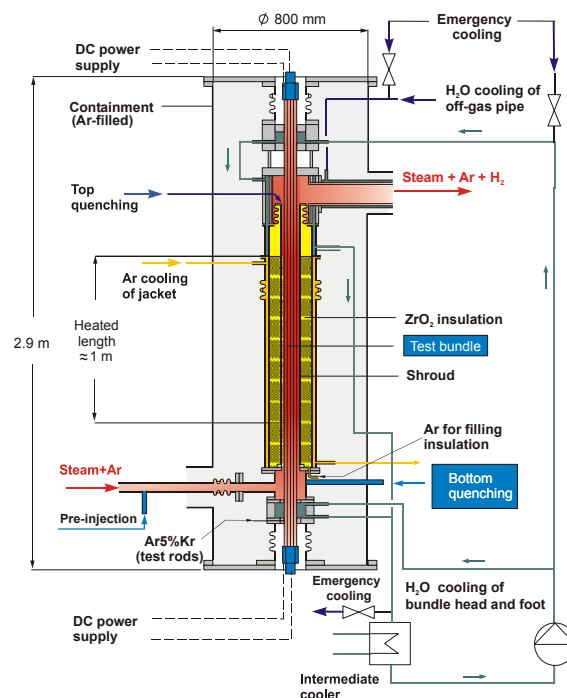


Fig. 1: The QUENCH test setup with its connections to the flow pipes.

1. INTRODUCTION

Cooling of an uncovered, overheated LWR (light water reactor) core with water is a prime accident management measure intended to terminate a severe accident transient. However, before the water succeeds in cooling the fuel elements, its injection may, under certain circumstances, cause renewed enhanced oxidation of the zircaloy cladding combined with a rapid increase in temperature and hydrogen generation because of the extensive exothermal zirconium-steam reaction. This phenomenon was demonstrated in analyses of the TMI-2 accident [1] and in results of out-of-pile, i.e. LWR and VVER, CORA bundle experiments [2-4] and in-pile, i.e. LWR, LOFT LP-FP-2 bundle experiments [5]. It is important that the hydrogen generation rate as a source term be known so that accident mitigation measures, e.g. passive autocatalytic recombiners, may be designed appropriately.

The QUENCH test facility at the Karlsruhe Research Center (Fig. 1) serves to investigate the hydrogen source term resulting from the injection of water or steam into an uncovered core, examine the physico-chemical behavior of overheated fuel elements under various flooding conditions, improve understanding of the effects of water injection at different stages of a degraded core, and create a database for model development and code improvement. The experiments are considered appropriate for the latter objective because of their relatively large scale and the possibility to compute temperatures and hydrogen buildup (in connection with cladding oxide scale growth) for the phases of a severe accident, before and during flooding of the rod bundle. From the so-called International Standard Problems (ISP), in which selected experiments were calculated with various severe-accident code packages within the CORA project [10, 11], to this day codes have improved significantly. The recent ISP of the QUENCH-06 test indicated the need for even further code improvement with respect to transient oxidation and reflooding simulation [12, 13].

These are the main parameters of the test program: quenching medium, i.e. water or steam, fluid injection rate; extent of cladding pre-oxidation at the onset of cooling; starting temperature for cooling. In the experiments performed so far, injection was from the bottom (see Table 1).

Table 1: Cooling parameters in the QUENCH experiments.

Test	Coolant	Injected mass flow rate	Injection period ^{a)}	Injection velocity
QUENCH-01 (Feb. 26, 98)	Water	52 g/s	89 s	1.7 cm/s ^{b)}
QUENCH-02 (July 7, 98)	Water	47 g/s	234 s	1.6 cm/s
QUENCH-03 (Jan. 20, 99)	Water	40 g/s	879 s	1.3 cm/s
QUENCH-04 (June 30, 99)	Steam	50 g/s	219 s	15-20 m/s ^{c)}
QUENCH-05 (March 29, 00)	Steam	50 g/s	286 s	15-20 m/s
QUENCH-06 (Dec. 13, 00)	Water	42 g/s	255 s	1.4 cm/s
QUENCH-07 (July 25, 01)	Steam	15 g/s	1550 s	4-6 m/s
QUENCH-09 (July 3, 02)	Steam	50 g/s	1175 s	15-20 m/s

a) Time between the first signal at the -250 mm level and termination of fluid injection.

b) For water: based on the injection flow rate and the coolant channel cross section of 30 cm², single-phase flow assumed.

c) Basis for steam: velocity at 400-600 K, 0.22 MPa.

As indicated above, the main results of the QUENCH experimental program are those on hydrogen generation (presented, e.g., in [8]). This paper discusses the temperature response during quenching (water injection) and cooling by steam (steam injection). As the facility was built for high-temperature tests under severe accident conditions, it was difficult to install extensive bundle instrumentation for two-phase flow, although it would be useful, e.g., to perform void measurements. The information obtained from rod and shroud thermocouples therefore is used to interpret the cooling behavior of the rod bundle.

2. TEST BUNDLE AND INSTRUMENTATION

The QUENCH test bundle is made up of 21 fuel rod simulators with a length of approximately 2.5 m. 20 fuel rod simulators are heated between axial levels 0 and 1024 mm. The one unheated fuel rod simulator is located in the center of the test bundle. Heating is electric by means of tungsten heater elements of 6 mm diameter installed in the center of the rods and surrounded by annular ZrO₂ pellets. The rod cladding is identical to that used in PWRs (pressurized water reactors): Zircaloy-4, 10.75 mm outside diameter, 0.725 mm wall thickness. The fuel rod simulators are held in position by five grid spacers, also identical to those in commercial PWRs. Four spacers are made of zircaloy; the one below the heated zone is made of inconel. The test bundle is surrounded by a 2.38 mm thick shroud of zircaloy, a 37 mm thick ZrO₂ fiber insulation, and a double-walled cooling jacket of stainless steel, as illustrated in the cross section of the test section in Fig. 2.

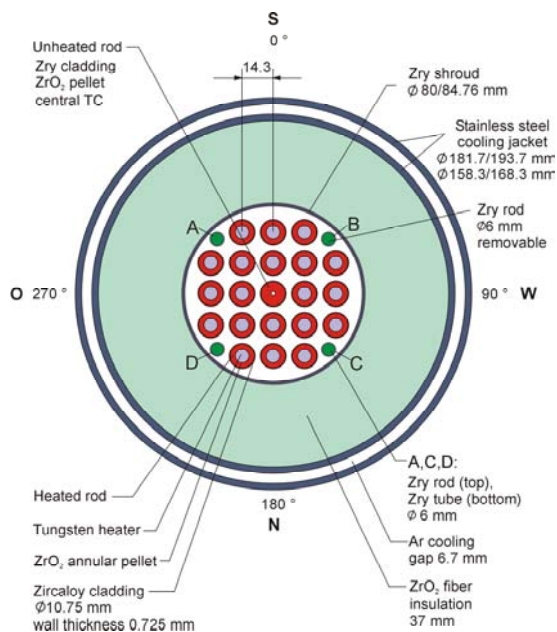


Fig. 2: Cross section (top view) of the fuel rod simulator bundle with shroud, insulation, and cooling jacket.

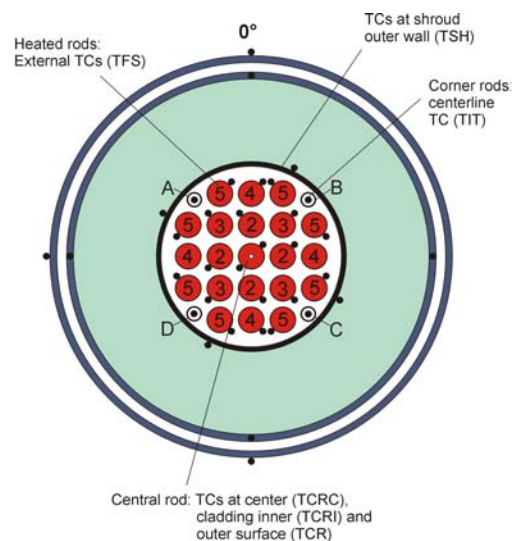


Fig. 3: Thermocouple positions of the test bundle, shroud, and corner rods together with their designations.

Prior to the cooling phase, superheated steam together with argon as the carrier gas enters the test bundle at the bottom and leaves it at the top together with the hydrogen produced in the zirconium-steam reaction. The gas composition is analyzed by three different instruments, of which the “GAM 300” Balzers mass spectrometer located at the offgas pipe, i.e. downstream of the test section, is the most important unit.

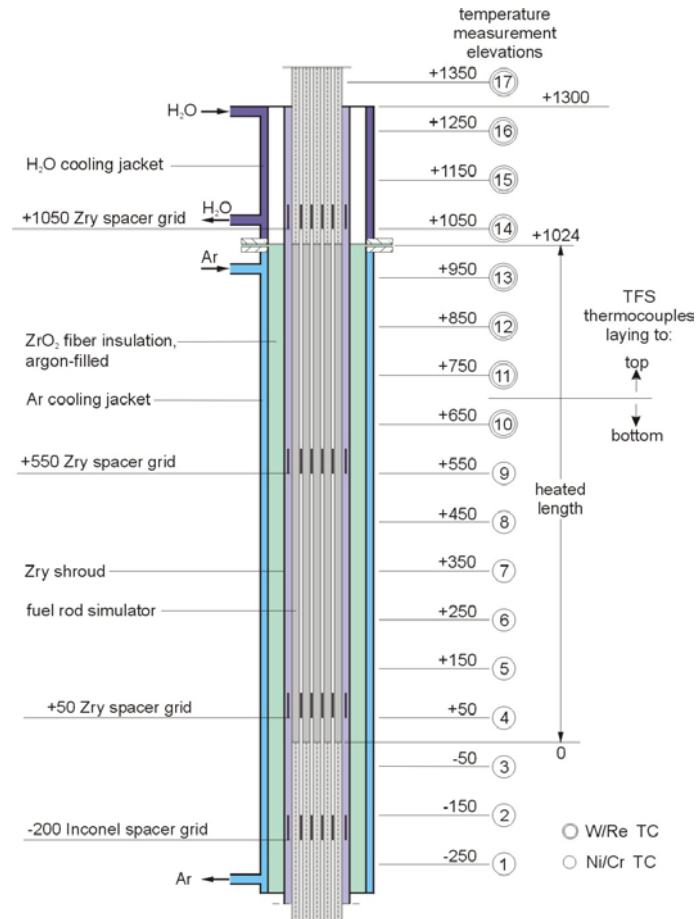


Fig. 4: Temperature measurement levels of the QUENCH test bundle and shroud. NiCr/Ni bundle thermocouples are used for measurement levels 1 through 9, while W/Re bundle thermocouples are used for measurement levels 10 through 17.

The test section is instrumented with thermocouples (TC) attached to the cladding, the shroud, and the cooling jackets at levels between -250 mm and 1350 mm. The azimuthal positions and designations of the thermocouples are given in Fig. 3, while the axial temperature measurement locations can be seen in the schematic in Fig. 4.

In the lower bundle region, i.e. up to the 550 mm elevation, NiCr/Ni thermocouples of 1 mm diameter are used for temperature measurements of the rod cladding, shroud, and corner rod. The thermocouples of the hot zone are high-temperature thermocouples with W-5Re/W-26Re wires, HfO₂ insulation, and a duplex sheath of tantalum (internal)/zircaloy with an outside diameter of 2.1 mm. The thermocouple attachment technique for the surface-mounted high-temperature TCs is illustrated in Fig. 5. The TC tip is held in place by two clamps of zirconium and – in case of pre-oxidation – additionally by an Ir-Rh wire.

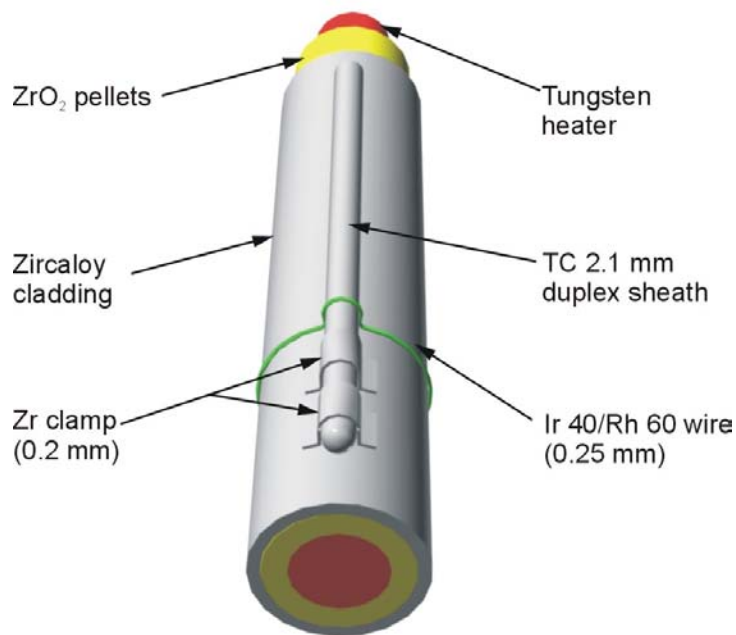


Fig. 5: Attachment of the surface-mounted high-temperature thermocouples by Zr clamps and an additional Ir-Rh wire (used only in case of pre-oxidation).

3. GENERAL TEST PROCEDURE

The QUENCH experiments comprise several test phases, i.e. heating, pre-oxidation (optional), transient, and quenching/cooling. All phases, except for the last one, are conducted in an argon/steam atmosphere at a flow rate of 3 g/s (each). In the transient phase, the heating rate starts at 0.1 K/s and increases to approx. 0.4 K/s at approx. 1400 K. The further increase in bundle heating depends on the evolution of the temperature excursion mainly caused by the exothermal zirconium-steam reaction. This temperature excursion usually begins at the 850-950 mm level approx. at 1770 K and leads to the maximum bundle temperature. From this level, the temperature excursion spreads downward and upward. Cooling is accomplished by injecting either water at saturation temperature (quenching) or saturated steam (steam cooling) instead of superheated steam at the bottom of the test section. The argon flow through the test section is switched over to the bundle head to continue providing a carrier gas for the hydrogen analysis systems during quenching. In tests QUENCH-01, -02, and -03, the quenching water is injected through a separate line at the high rate of 80-90 g/s for some 25 s to fill the lower plenum of the test section. Once the lower plenum has been filled, the water injection flow is reduced to the target rate of 40-50 g/s. In the QUENCH-06 test, a pre-injection system was added to the test facility to shorten the time required to fill the pipes and the lower plenum of the test section, i.e., in this experiment, 4 kg of quenching water were pre-injected into the inlet pipe for 5 s.

To initiate the steam cooling sequence, the flow of 3 g/s of superheated steam is turned off, the cooling steam is injected at a rate of 50 or 15 g/s at the bottom of the test section, and the argon carrier gas flow remains unchanged. For both water and steam injection: (1) The flow rate is held constant until the bundle temperature has reached ~400-500 K; (2) approximately 25 s after cooling initiation the electric bundle power is reduced from its maximum level of approx. 20 kW to 4 kW to simulate a decay heat level.

4. EXPERIMENTAL RESULTS AND DISCUSSION

4.1 Test Bundle Behavior during Quenching with Water

At the initiation of the reflooding phase, the cladding temperatures of the rods are above 2000 K at the axial levels 750-1000 mm. “Onset of cooling” is detected as a first response of the TFS 2/1 coolant thermocouple positioned at the -250 mm level. As the water level reaches the lower bundle plenum and starts to rise around the hot rods, complex heat transfer processes develop under two-phase flow conditions. The injected water which is already at saturation at the inlet of the test section, i.e. at ~ 400 K, 0.2 MPa, contacts the hot bundle structure and starts to evaporate. The steam preceding the quenching front has a high velocity and causes the thermocouples on the outer rod surface to signal the onset of cooling at the lower bundle levels within a second. According to the temperature measurements at the rod cladding and the shroud, the test bundle is cooled in two stages, namely in a moderate cooling step (with heat transferred by film boiling) followed by a period of pronounced cooling (heat transfer by transition and nucleate boiling). The two cooling stages can be seen at the 150 mm, 550, and 950 mm elevation of test QUENCH-06 in Fig. 6.

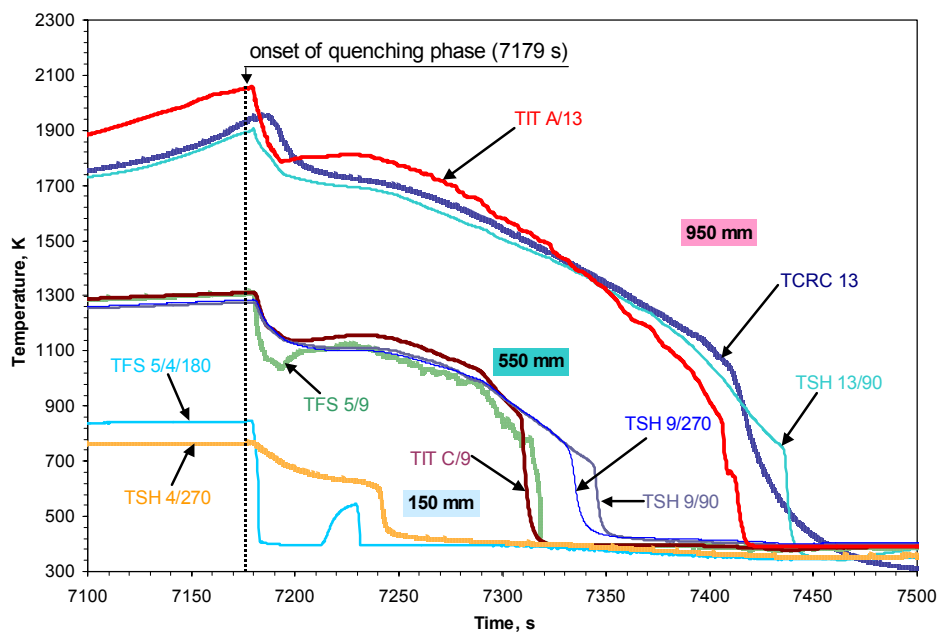


Fig. 6: Temperature response of the TFS (rod outer surface), TCRC (central rod centerline), TIT (corner rod centerline), and TSH (shroud) thermocouples during quenching with water (QUENCH-06) at three different levels.

In Fig. 6, thermocouple TFS 5/4/180 shows a temperature rise some 35 s after the onset of the quenching phase. This rise is followed by a sudden temperature drop reflecting the onset of the “main quenching” phase (after a stagnation between the fast pre-injection and main injection periods). The sequence of fast injection for ~ 5 s at 800 g/s, no water injection for ~ 20 s, and main injection at 42 g/s can also be seen at the 550 and 950 mm levels in Fig. 6. The cooling phase in the upper half of the bundle remains moderate over a prolonged period of time (see 950 mm level). Nevertheless, the upper levels exhibit similar temperature behavior, but the stage of pronounced cooling is clearly delayed.

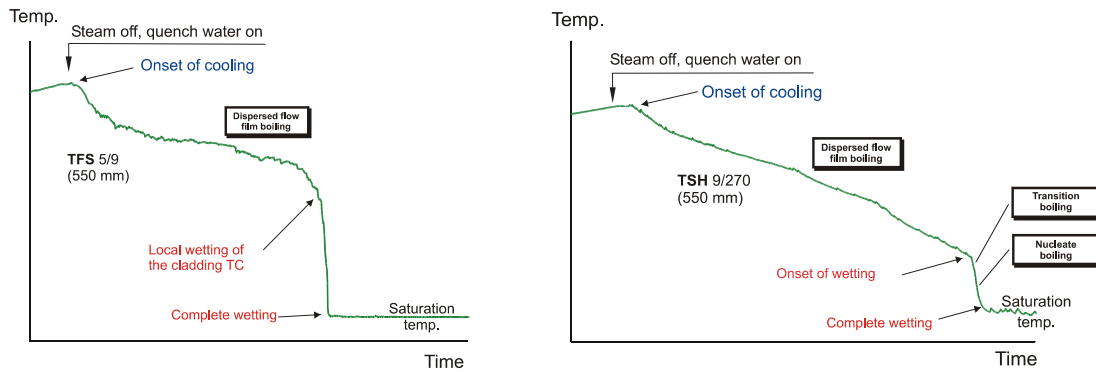


Fig. 7: Typical temperature response of an externally mounted cladding thermocouple (type TFS, left) compared to that of a shroud thermocouple (type TSH, right) during quenching with water (QUENCH-03), schematic, together with the pertinent flow regimes.

The onset of rapid cooling as indicated by the cladding thermocouples of the TFS type at the three levels in Fig. 6 can be regarded as a first wetting. This “wetting point,” however, is considered to be local, and its temperature seems too high for real wetting. The QUENCH experiments showed that TFS-type thermocouples are preferable for the transient phase, as they indicate the test rod temperature quite correctly. (To account for the deviation of external surface TCs, the central rod of the QUENCH-06 bundle was equipped with TCs on the cladding inner surface and in the rod center at 350 mm and 550 mm in addition to the TCs on the cladding outer surface.) The differences of internal and external rod cladding temperatures turned out to be relatively small during the transient, i.e. in the steam-argon atmosphere (3 g/s + 3 g/s). In the temperature range of 1020–1320 K, during the transient of test QUENCH-06, the internal and the pertinent external cladding thermocouples showed temperature differences of 17-19 K for the axial level of 550 mm [9]. (During the transient of test QUENCH-04, temperature differences were 8-30 K.)

At the beginning of cooling, however, the rod outer surface (TFS-type) thermocouples do not measure correctly [7]. They indicate complete wetting of the rod when the first droplets contact the thermocouple sheaths. The shroud thermocouples (TSH, see Fig. 3) are not exposed to the coolant flow, being mounted outside the coolant channel. The shroud thermocouples indicate the onset of wetting, according to the definitions given in Fig. 7, to lie in the range of 600-800 K, i.e. at a lower temperature than shown in the TFS thermocouple traces, but still too high with respect to the Leidenfrost temperature of approx. 500 K. The temperatures of the shroud thermocouples, however, unfortunately are delayed by a considerable margin as can be seen in Fig. 6.

After the “onset of wetting,” the wetting process goes on during the stage of rapid cooling stage which is characterized by the maximum surface heat flux (nucleate boiling heat transfer) and is completed when the temperature drops below the saturation level. Heat transfer then takes place by conduction and convection and is considerably reduced compared to heat transfer by nucleate boiling. The TFS response can only reflect the regime of heat transfer by film boiling (moderate cooling phase) and complete wetting (when the temperature is below the saturation level). The TSH response in addition is able describe the onset of wetting and the heat transfer regimes of transition and nucleate boiling (indicated in Fig. 7).

The heat transfer conditions during quenching with water are described in [6]. They are based on current knowledge and can be summarized as follows: During the phase of moderate cooling, inverted annular film boiling exists downstream of the quench front. This phase is characterized by a steam film covering the rod surface and separating the flow of large liquid lumps. Heat is transferred by convection from the rod surface to the steam and on to the water

droplets. In addition, heat is transferred directly from the hot surface to the water by radiation. With the water level rising, the flow regime proceeds to dispersed-flow film boiling where water droplets are entrained in the bulk steam. The phase of moderate cooling is followed by a period of pronounced cooling associated with the collapse of the stable steam film. Heat transfer is characterized by transition and nucleate boiling, particularly at the wetting front.

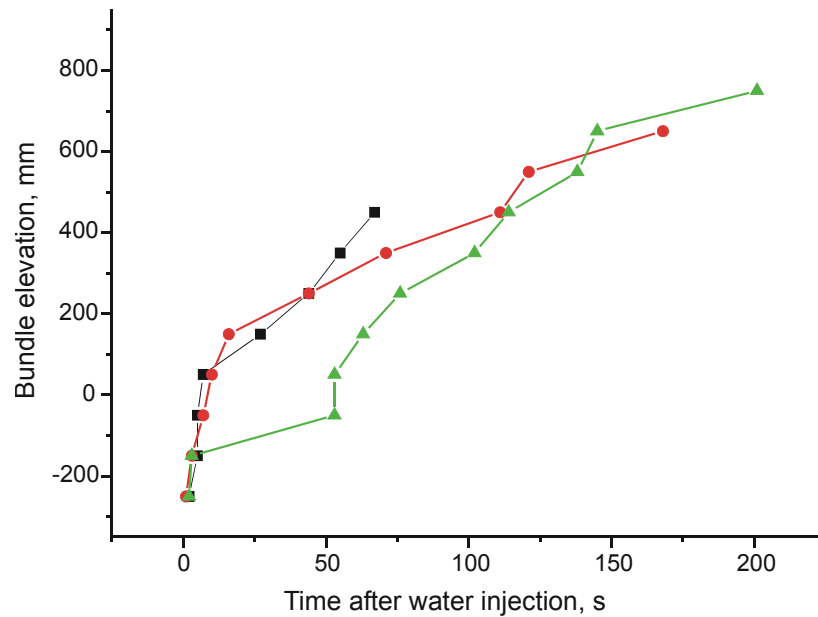


Fig. 8: Progression of the wetting front in the QUENCH-01 (square symbols), QUENCH-03 (full circle), and QUENCH-06 (triangle) water injection experiments based on the first indication of saturation temperature by the cladding surface thermocouples (TFS).

Evaluation of the progression of the wetting front was based on the evolution of complete wetting in the axial direction, i.e. the first indication of saturation temperature. Figure 8 presents the rise of the wetting front during the flooding phase of experiments QUENCH-01, -03, and -06 based on the cladding surface temperature data (TFS) and plotted as elevation versus time after the onset of water injection. In the QUENCH-01, -03, and -06 experiments, the wetting front progresses at a velocity of approx. 0.5-0.6 cm/s from 50 to 500 mm. The rates of rise are similar for the QUENCH-01 and -03 experiments. The data of QUENCH-06 deviate from the other data approximately up to the 250 mm level. As described above, prompt cooling of the test bundle starts after fast water pre-injection. As a consequence, the cladding temperature drops to the saturation temperature of approx. 400 K at axial levels of up to 250 mm. 35 s later the cladding temperatures rise again due to evaporation of the pre-injected water at the bottom of the test section. The increase in bundle temperature is followed by the main cooling phase, with the same water flow rate used in the QUENCH-01 and -03 experiments.

One of the important results of the QUENCH experiments is the progression of the water front. This is determined by the liquid level indicator, L 501, a differential pressure, (Δp), measurement between the bottom and the top of the bundle. In Fig. 9, these results are compared with the data obtained from the wetting data of the cladding surface (TFS) and shroud (TSH) thermocouples in experiments QUENCH-01 and -06 to demonstrate the ability of L 501 to represent the progression of the water front acceptably. The QUENCH-01 bundle was filled to ~600 mm, while the QUENCH-06 bundle was filled to the top (for QUENCH-06, only the main injection period is plotted), which is in agreement with the shape of the Δp curve.

Even though the uncertainties in the L 501 measurements are rather large, the results can be used to evaluate adequately the progression of the quench front in the QUENCH experiments.

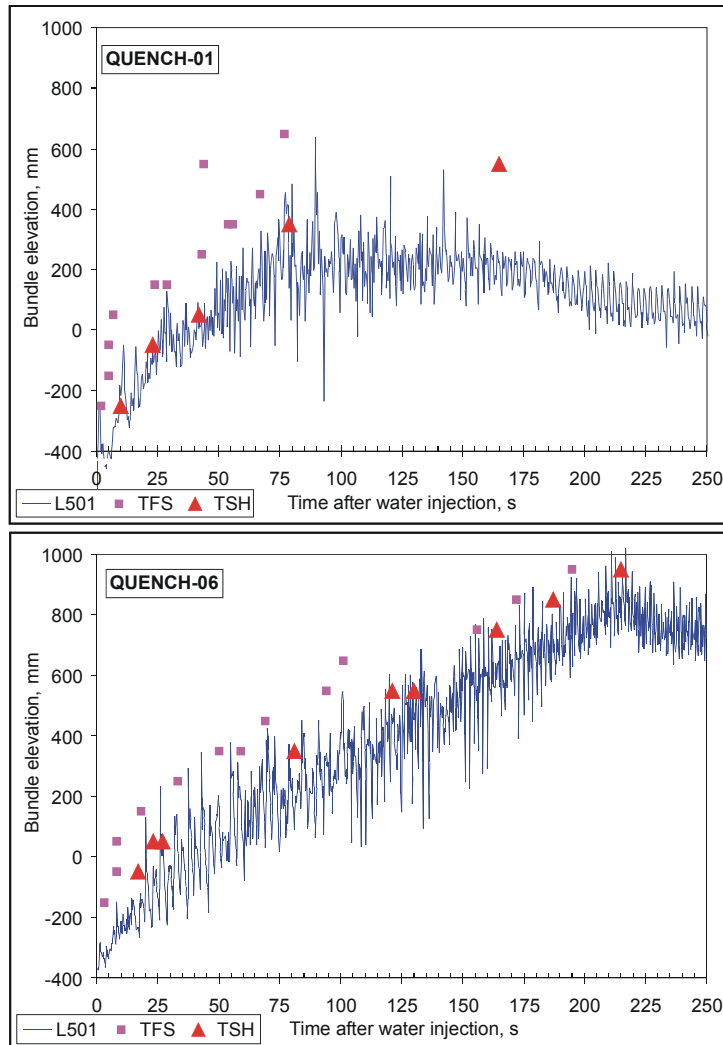


Fig. 9: Comparison of the rise of the water level between experiments QUENCH-01 (top diagram, bundle filled to ~600 mm) and QUENCH-06 (lower diagram, bundle filled to the top), based on measurements of the liquid level indicator L 501, the cladding surface thermocouples (TFS), and the shroud temperature data (TSH).

4.2 Test Bundle Behavior during Cooling by Steam

The initial conditions at the starting point of cooling by steam are similar to those for water injection, i.e. the rod cladding temperatures are above 2000 K at the axial levels of 750-1000 mm. Due to the one-phase flow conditions, cooling by steam exhibits continuous cooling behavior throughout the cooling phase. This can be seen in Fig. 10 for test QUENCH-04.

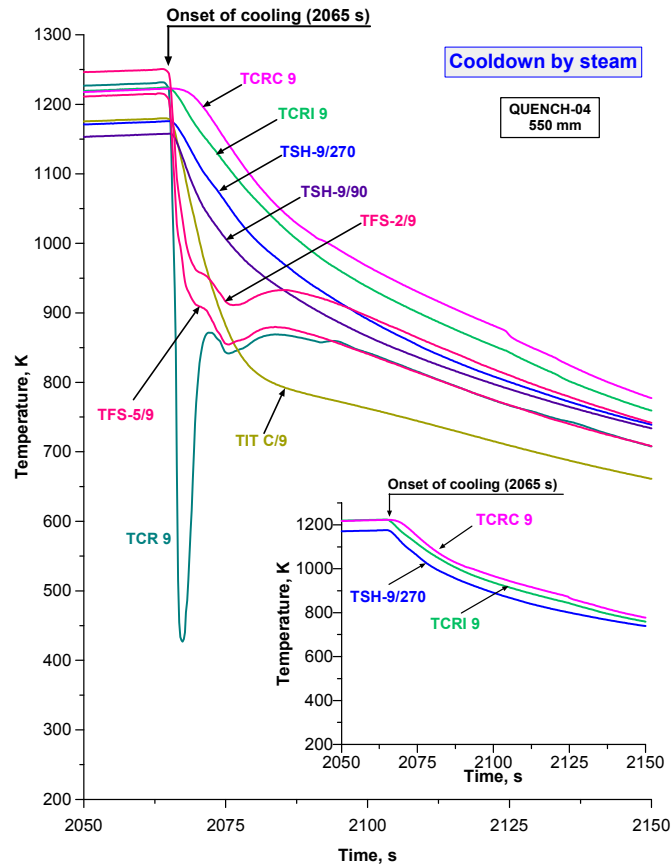


Fig. 10: Typical temperature response of the TFS, TCR, TCRC, TIT, and TSH thermocouples at the 550 mm level during cooling by steam (QUENCH-04). In the inset of this figure, the externally mounted cladding thermocouples are omitted so that the TCRC and TCRI (internal thermocouples of the central rod) and TSH (shroud outer wall TC) temperature traces are compared.

The high steam velocity of 15-20 m/s (relative to an injection rate of 50 g/s, a steam temperature of 400-600 K and a coolant channel cross section of 30 cm²) leads to a fast response of the thermocouples at the very beginning of the cooling process, as is demonstrated clearly by the externally mounted thermocouples, TFS 2/9, TFS 5/9, TCR 9 in Fig. 10. Particularly the sharp drop of thermocouple TCR 9 can be explained by droplets stemming from local condensation of the steam in the inlet line, which shows at the onset of the cooling phase. The internal thermocouples of the central rod (TCRC and TCRI) do not show the sudden decrease toward the saturation temperature level, which is seen more clearly in the inset of this figure.

In Fig. 11, the temperature responses of the shroud thermocouples during cooling by water and steam are compared at 550 mm. Differences are most evident at 550 mm: The water-quenching experiments, QUENCH-01, -02, -03, and -06, exhibit the “two-stage” cooling behavior of the rod bundles as described above. Temperatures recorded in the QUENCH-04, -05, -07, and -09 steam injection tests exhibit a fast response in the beginning, due to the high steam velocity in connection with the outside location of the thermocouples (fin cooling effect and/or local condensation at the thermocouple). Afterwards, cooling is moderate so that the 400 K level is reached significantly later than in the case of water quenching. At the upper levels, though, differences between water and steam injection become less due to similar atmospheres (predominantly steam for most of the time). The QUENCH-07 temperature does not drop as fast compared to the other steam injection tests, because the injection rate was lower, i.e. 15 instead of 50 g/s.

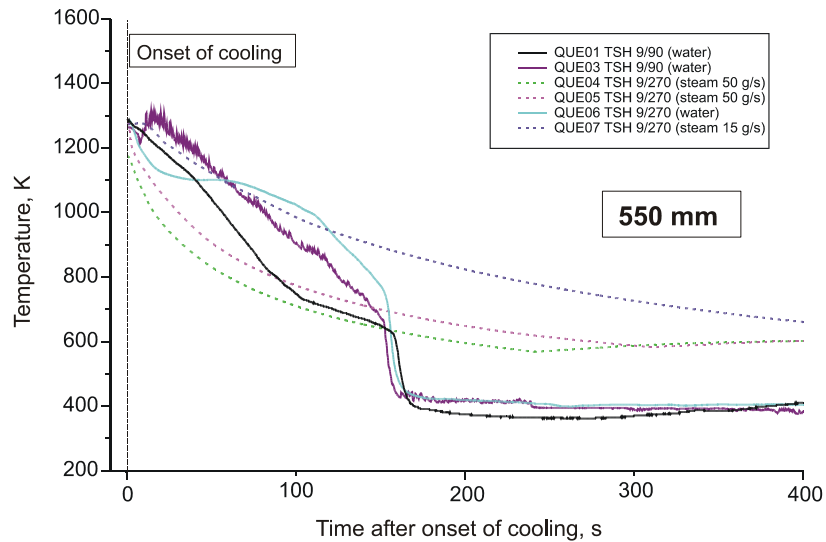


Fig. 11: Comparison of cooling behavior during tests QUENCH-01 through QUENCH-09 at 550 mm using shroud temperature data.

4.3 Quenching Water Evaporation Rate

To evaluate evaporation during quenching, data from three independent instruments were evaluated for the QUENCH-06 experiment: (1) mass spectrometer measurement (MS steam), (2) differential pressure data of the F 601 standard orifice located in the offgas pipe, and (3) L 701 condensate collector data.

The steam mass flow rates as assessed by the three different methods are compared with each other, and with the quenching water feed, F 104, in Fig. 12. In addition, an average of the three curves by a rough approximation (thick solid line in the diagram) is presented as mean steam flow data. These mean data indicate that the 42 g/s of water injected were turned into approx. 30 g/s of steam at the beginning of the cooling phase, decreasing to a fairly constant steam flow rate of 15 g/s from 70-80 s after quench initiation. So, the ratio of mass rates of steam produced to water injected seems to change mainly during the first period of the quenching phase. The peaks at the beginning of flooding (7179 s) indicated by the three instruments can be explained by the fast injection described above, preceding injection at 42 g/s, as indicated by F 104. (Pre-injection cannot be seen from the F 104 quenching water flow as it is measured upstream of the test section inlet.) The peak in the derivative of the L 701 data is delayed due to the location of the condensate collector tank. The low MS steam data after the peak could be caused by some condensation in the MS sampling line. After 70-80 s, however, agreement among the three data histories seems to be quite satisfactory.

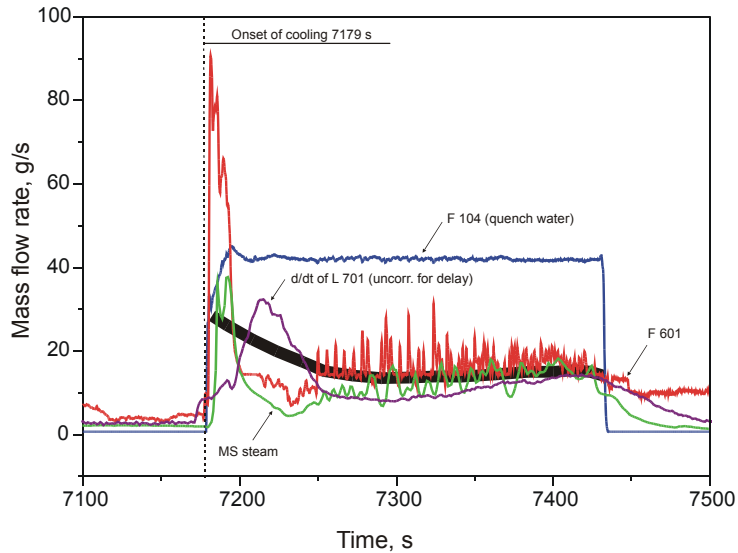


Fig. 12: Steam flow measurements in the offgas pipe (MS steam, F 601), in the condensate collector ($d(L\ 701)/dt$), and mean steam flow data (thick solid black line) are compared to the quenching water feed, F 104, vs. time in test QUENCH-06. The mean data are meant to reflect an evaporation rate during the quenching phase.

4.4 Cooling Rates

Cooling rates, $(T_1 - T_2)/(t_1 - t_2)$, were evaluated on the basis of the shroud temperature data. These rough cooling rates are merely meant for comparing the cooling behavior of the test rod bundles in the various QUENCH experiments and cannot be extrapolated to fuel elements of power plants. Also, local effects of temperature escalation are not considered in this method.

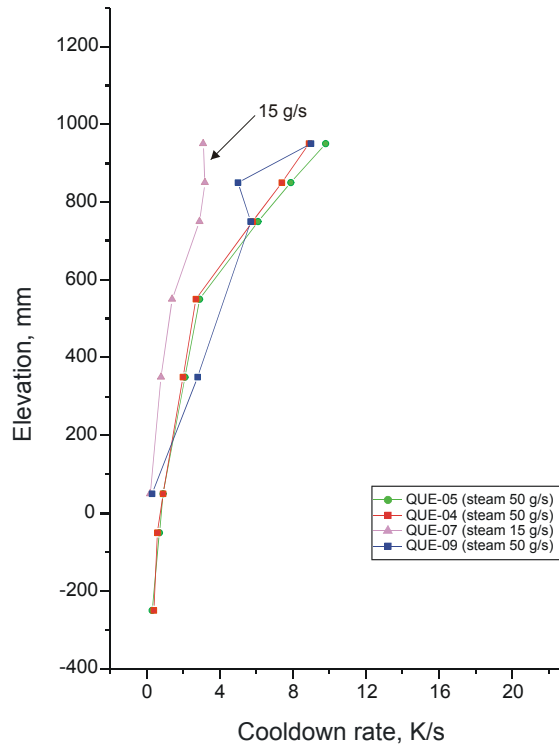


Fig. 13: Influence of the steam flow rate on the mean cooling rates, $(T_1 - T_2)/(t_1 - t_2)$, of the QUENCH experiments, i.e. 15 vs. 50 g/s. The drop in shroud temperature to half its initial value per unit time ($T_2 = 0.5 T_1$) is plotted versus the axial level.

Due to the different heat transfer regimes existing in the water quenching experiments, cooling rates of tests QUENCH-01, -03 and -06 were evaluated separately for the different cooling phases, i.e. for the first cooling phase (inverted annular film boiling) and for the wetting phase (transition and nucleate boiling). No different phases must be considered during cooling with steam. The procedure for experiments QUENCH-04, -05, -07 and -09 is identical, i.e. the drop in the shroud temperature from the maximum to half its initial level ($T_2 = 0.5 T_1$) was chosen for evaluation of the mean cooling rates at different bundle levels. As expected, the results show differences for water and steam injection, and for the different heat transfer regimes during quenching with water as well. During film boiling, the cooling rate amounts to 3-20 K/s due to the poor thermal conductivity of the steam. During nucleate boiling, rates are 40-100 K/s for the lower part of the bundle, and 10-60 K/s for the upper part of the bundle, i.e. above the 750 mm level.

The cooling rates during steam injection as a function of the level are given for the heated zone, i.e. up to 950 mm, in Fig. 13. The rates are 2-12 K/s and, therefore, are only slightly lower than those for film boiling in the water quenching tests (3-20 K/s) at comparable injection rates. This is to be expected, for the heat transfer coefficients are similar for film boiling and single-phase steam cooling. The cooling rates usually rise with higher axial levels due to the higher temperature at the starting point of the injection. In addition, Fig. 12 also shows the effect of a lower injection rate as used in test QUENCH-07, i.e. 15 instead of 50 g/s.

SUMMARY

- At the onset of the cooling phase, the temperature was at its maximum in four experiments. In the other four QUENCH tests, temperature and hydrogen release increased significantly despite the high rate of water or steam injection.
- In the water injection experiments the test bundle is cooled under two-phase flow conditions in two stages: a moderate cooling phase (film boiling regime) and a rapid cooling phase (transition or nucleate boiling regime).
- In the upper half of the bundle, i.e. downstream of the quenching front, the onset of local wetting is delayed so that film boiling prevails throughout most of the cooling phase.
- The starting point for rapid cooling is considered the onset of local wetting, whereas complete wetting of the rod surfaces occurs later in time, i.e. when heat is transferred from the bundle to the coolant by nucleate boiling.
- In the steam-injection tests, cooling is less complex because of single-phase flow conditions. The temperature decreases continuously in one step.
- Evaluation of the evaporation rate in test QUENCH-06 indicates that, from 70-80 s after quench initiation, the steam production decreased to a more or less constant rate of roughly 35 % (relative to the injected water of 42 g/s).
- The wetting front evaluated for the QUENCH-01, -03, and -06 experiments rises at a velocity of approx. 0.5-0.6 cm/s from 50 to 500 mm.

CONCLUSION

The main objective of the QUENCH experimental program is the investigation of hydrogen buildup during severe bundle degradation. The thermohydraulics of the test bundle play an important role for the results of cladding oxidation and hydrogen production. Despite the lack of special two-phase flow instrumentation, thermocouple instrumentation can be used to a certain extent to evaluate boundary conditions of the tests. So, the experiments are considered suitable for establishing a database for model development and code improvement because of the relatively large scale of the test facility and the possibility to compute temperatures and hydrogen buildup (in connection with cladding oxide scale growth) for the different phases of a severe accident, i.e. before and during flooding of the rod bundle.

ACKNOWLEDGMENTS

Dr. P. Hofmann initiated the QUENCH experimental program at the Karlsruhe Research Center and set its main direction by guiding the first experiments. The QUENCH-01, -02, -07, and -09 tests were co-financed by the Fifth Framework Programme of the European Community for Research, Technological Development and Demonstration Activities (1998 to 2002).

The authors would like to thank in particular Messrs. S. Horn, J. Moch, and R. Vouriot for assembling and instrumenting the test bundle, Mr. L. Schmidt for operating the test facility during the first experiments, Mr. D. Piel for test data acquisition, Mrs. J. Laier and Mrs. M. Heck for test data processing. Thanks are also due to Dr. A. Palagin for discussions of this paper, and to Mrs. I. Werner for formatting the text and figures of this paper.

REFERENCES

1. J.M. Broughton, P. Kuan, and D.A. Petti, "A Scenario of the Three Mile Island Unit 2 Accident," *Nuclear Technology*, 87, 34, 1989.
2. P. Hofmann, S. Hagen, V. Noack, G. Schanz, L. Sepold, "Chemical-Physical Behavior of Light Water Reactor Core Components Tested under Severe Reactor Accident Conditions in the CORA Facility," *Nuclear Technology*, vol. 118, 1997, p. 200.
3. S. Hagen, P. Hofmann, V. Noack, L. Sepold, G. Schanz, G. Schumacher, "Comparison of the Quench Experiments CORA-12, CORA-13, CORA-17," FZKA 5679, Forschungszentrum Karlsruhe, 1996.
4. S. Hagen, F. Seibert, L. Sepold, P. Hofmann, G. Schanz, G. Schumacher, „Influence of Reflood in the CORA Severe Fuel Damage Experiments," *Proceedings of the National Heat Transfer Conference*, Minneapolis, 1991, American Institute of Chemical Engineers, ISBN 0-8169-0548-7
5. S.M. Modro and M.L. Carboneau, "The LP-FP-2 Severe Fuel Damage Scenario; Discussion of the Relative Influence of the Transient and Reflood Phase in Affecting the Final Condition of the Bundle," OECD/LOFT Final Event, ISBN 92-64-03339-4, 1991, p. 388.

6. L. Sepold, P. Hofmann, W. Leiling, A. Miassoedov, D. Piel, L. Schmidt, M. Steinbrück, "Reflooding Experiments with LWR-Type Fuel Rod Simulators in the QUENCH Facility," *Nuclear Engineering and Design* 204 (2001), 205-220.
7. L. Sepold, P. Hofmann, W. Leiling, A. Miassoedov, D. Piel, L. Schmidt, M. Steinbrück, "Reflood Behavior of PWR-Type Rod Simulators used in the QUENCH Experiments," *Proceedings of the 33rd National Heat Transfer Conference*, Albuquerque, NM, Aug. 15 – 17, 1999.
8. L. Sepold, C. Homann, A. Miassoedov, G. Schanz, U. Stegmaier, M. Steinbrück, J. Stuckert, "Hydrogen Generation in Reflood Experiments with LWR-type Rod Bundles (QUENCH Program)," Transactions of the ANS Annual Meeting San Diego, CA, June 1-5, 2003, to be published.
9. L. Sepold, C. Homann, A. Miassoedov, G. Schanz, U. Stegmaier, M. Steinbrück, H. Steiner, "Experimental and Computational Results of the QUENCH-06 Test (OECD ISP-45)," FZKA 6664, Forschungszentrum Karlsruhe, to be published.
10. S. Hagen, P. Hofmann, V. Noack, G. Schanz, G. Schumacher, L. Sepold, "Results of SFD Experiment CORA-13 (OECD International Standard Problem 31)," KfK 5054, Forschungszentrum Karlsruhe, 1993.
11. M. Firnhaber, S. Yegorova, U. Brockmeier, S. Hagen, P. Hofmann, K. Trambauer, "International Standard Problem ISP36, CORA-W2 Experiment on Severe Fuel Damage for a Russian Type PWR, Comparison Report," GRS-120, FZKA 5711, OECD/GD(96)19, ISBN 3-923875-81-9, 1996.
12. W. Hering, C. Homann, J.-S. Lamy, "Comparison Report on the blind phase of the OECD International Standard Problem No. 45 Exercise (QUENCH-06)," FZKA 6677, Forschungszentrum Karlsruhe, 2002.
13. W. Hering, C. Homann, J.-S. Lamy, A. Miassoedov, G. Schanz, L. Sepold, M. Steinbrück, "Comparison and Interpretation Report of the OECD International Standard Problem No. 45 Exercise (QUENCH-06)," FZKA 6722, Forschungszentrum Karlsruhe, 2002.